

# Potent Antitumor Activity of a Novel Cationic Pyridinium-Ceramide Alone or in Combination with Gemcitabine against Human Head and Neck Squamous Cell Carcinomas in Vitro and in Vivo

Can E. Senkal, Suriyan Ponnusamy, Michael J. Rossi, Kamala Sundararaj, Zdzislaw Szulc, Jacek Bielawski, Alicja Bielawska, Mario Meyer, Bengu Cobanoglu, Serap Koybasi, Debajyoti Sinha, Terry A. Day, Lina M. Obeid, Yusuf A. Hannun, and Besim Ogretmen

*Departments of Biochemistry and Molecular Biology (C.E.S., S.P., K.S., Z.S., J.B., A.B., B.C., L.M.O., Y.A.H., B.O.), Hollings Cancer Center (A.B., M.M., T.A.D., L.M.O., Y.A.H., B.O.), Otolaryngology and Head and Neck Surgery (M.J.R., S.K., T.A.D.), Biostatistics, Bioinformatics, and Epidemiology (D.S.), and Medicine and Ralph H. Johnson Veterans Administration Hospital (L.M.O.), Medical University of South Carolina (MUSC), Charleston, South Carolina*

Received January 27, 2006; accepted February 28, 2006

## ABSTRACT

In this study, a cationic water-soluble ceramide analog *L*-*threo*-C<sub>6</sub>-pyridinium-ceramide-bromide (*L*-t-C<sub>6</sub>-Pyr-Cer), which exhibits high solubility and bioavailability, inhibited the growth of various human head and neck squamous cell carcinoma (HNSCC) cell lines at low IC<sub>50</sub> concentrations, independent of their p53 status. Consistent with its design to target negatively charged intracellular compartments, *L*-t-C<sub>6</sub>-Pyr-Cer accumulated mainly in mitochondria-, and nuclei-enriched fractions upon treatment of human UM-SCC-22A cells [human squamous cell carcinoma (SCC) of the hypopharynx] at 1 to 6 h. In addition to its growth-inhibitory function as a single agent, the supra-additive interaction of *L*-t-C<sub>6</sub>-Pyr-Cer with gemcitabine (GMZ), a chemotherapeutic agent used in HNSCC, was determined using isobologram studies. Then, the effects of this ceramide, alone or in combination with GMZ, on the growth of UM-SCC-22A xenografts in SCID mice was assessed following the determination of preclinical parameters, such as

maximum tolerated dose, clearance from the blood, and bioaccumulation. Results demonstrated that treatment with *L*-t-C<sub>6</sub>-Pyr-Cer in combination with GMZ significantly prevented the growth of HNSCC tumors in vivo. The therapeutic efficacy of *L*-t-C<sub>6</sub>-Pyr-Cer/GMZ combination against HNSCC tumors was approximately 2.5-fold better than that of the combination of 5-fluorouracil/cisplatin. In addition, liquid chromatography/mass spectroscopy analysis showed that the levels of *L*-t-C<sub>6</sub>-Pyr-Cer in HNSCC tumors were significantly higher than its levels in the liver and intestines; interestingly, the combination with GMZ increased the sustained accumulation of this ceramide by approximately 40%. Moreover, treatment with *L*-t-C<sub>6</sub>-Pyr-Cer/GMZ combination resulted in a significant inhibition of telomerase activity and decrease in telomere length in vivo, which are among downstream targets of ceramide.

Human head and neck squamous cell carcinomas (HNSCCs) are among the five most common cancers in the world. Global

This work was supported by the National Institutes of Health (Grants CA88932 and DE01657 to B.O., CA097132 to Y.A.H., and AG16583 to L.M.O.), by the Department of Defense (Phase VII Program Project Grant through Hollings Cancer Center to B.O.), and by the National Science Foundation/Experimental Program to Stimulate Competitive Research (Grant EPS-0132573 to B.O.). The animal facility used in this study was supported by the National Institutes of Health (Grant C06 RR015455 to MUSC) from the Extramural Research Facilities Program of the National Center for Research Resources.

Article, publication date, and citation information can be found at <http://jpet.aspetjournals.org>.  
doi:10.1124/jpet.106.101949.

occurrence of HNSCC is high, and it is estimated that approximately 780,000 new patients are diagnosed with HNSCC each year in the adult population. There are approximately 41,000 new HNSCC cases diagnosed annually in the United States in 2004, and the overall 5-year survival of patients with stage III and IV disease remains less than 50% (Her, 2001; Jemal et al., 2004).

Historically, chemotherapy did not play a curative role in the treatment of HNSCC but was reserved for palliative therapy. Surgery and radiation therapy remained the primary curative options; however, complications of these ther-

**ABBREVIATIONS:** HNSCC, human head and neck squamous cell carcinoma; CP, cisplatin; 5-FU, 5-fluorouracil; *L*-t-C<sub>6</sub>-Pyr-Cer, *L*-*threo*-C<sub>6</sub>-pyridinium-ceramide-bromide; GMZ, gemcitabine; UM-SCC-22A, human squamous cell carcinoma of the hypopharynx; MUSC, Medical University of South Carolina; MS, mass spectroscopy; LC, liquid chromatography; MTT, 3-(4,5-dimethylthiazol-2-yl)-2,5-diphenyltetrazolium; MTD, maximum tolerated dose; bp, base pair(s); hTERT, human telomerase reverse transcriptase; PCR, polymerase chain reaction; TRAP, telomere repeat amplification protocol; Q-PCR, quantitative PCR; TRF, telomere restriction fragment.

apies resulted in significant morbidity and cosmetic deformity along with the inability to speak, swallow, or chew. There is now increasing evidence that treatment combinations including chemotherapy offer improved cure rates compared with standard therapies. Conventional chemotherapy of HNSCC in the clinic involves mainly the combination of cisplatin (CP) with 5-fluorouracil (5-FU) or taxol (Argiris et al., 2004; Cohen et al., 2004). Recent studies have evaluated the combination of gemcitabine with a variety of anticancer agents such as vinorelbine, imatinib, or cisplatin with limited pharmacokinetic or synergistic interaction (Airoldi et al., 2003; Bruce et al., 2005; Jiang et al., 2005). Radiosensitization property of GMZ was also examined in patients with advanced HNSCC, and the data showed that the concurrent use of radiotherapy and gemcitabine was effective but caused severe mucositis in the majority of patients (Aguilar-Ponce et al., 2004). Combination therapy involving anthracyclines against these cancers has also been analyzed previously, with strict adherence to the dose limitations of these cardiotoxic compounds (Harrington et al., 2001). Despite these new treatment options, however, survival statistics for HNSCC have not improved significantly in decades (Her, 2001; Jemal et al., 2004). Therefore, the development of novel strategies is needed for the treatment of HNSCC.

The bioactive sphingolipid ceramide, an emerging tumor suppressor lipid, is known to regulate antiproliferative responses, such as apoptosis, growth arrest, differentiation, and senescence in various human cancer cells (Ogretmen and Hannun, 2004). Many important biological targets and signaling events regulated by ceramide have been identified (Ogretmen and Hannun, 2004). Among these, telomerase activity has been detected in the majority of HNSCC tumors and not in normal adjacent tissues (Fabricius et al., 2002; Koscielny et al., 2004). Moreover, increased telomerase activity in the tumors of HNSCC patients has been associated with high cell proliferation rates, and advanced pathologic stage (Patel et al., 2002), demonstrating that telomerase activity is one of the most important prognostic factors in HNSCC patients and that telomerase can be an important target to develop novel therapeutic strategies for the treatment of these cancers (Tao et al., 2005).

Because of its antiproliferative roles, exogenous ceramide has been used for the treatment of various human cancer cells both in vitro and in vivo. However, this approach presents some major challenges due to its very low water solubility and moderate/low cellular uptake, intracellular metabolism to complex sphingolipids, and uncontrolled delivery, release, and intracellular targeting. To overcome these problems, many biophysical and chemical approaches have been developed with improved delivery and bioavailability (Shabbits and Mayer, 2003; Stover and Kester, 2003). Another alternative approach has been the development of novel pyridinium ceramide analogs with increased water solubility, cell membrane permeability, and cellular uptake compared with their uncharged conventional ceramides (Novgorodov et al., 2005; Rossi et al., 2005). Pyridinium ceramides are designed to preferentially localize into negatively charged intracellular compartments, specifically mitochondria and nucleus, due to the presence of a positive charge delocalized over the  $\pi$ -electron system. The accumulation of *D-erythro*-C<sub>6</sub>-Pyr-Cer specifically in mitochondria has been confirmed recently, and

the data showed that mitochondrial localization of Pyr-Cer caused a decrease in its membrane potential, leading to cytochrome C release and apoptosis (Novgorodov et al., 2005). In another independent study, antiproliferative responses of L-t-C<sub>6</sub>-Pyr-Cer, such as inhibition of cell cycle and telomerase activity, in HNSCC cell lines, but not in noncancerous human adult keratinocytes and Wi-38 lung fibroblasts, were demonstrated (Rossi et al., 2005). The improved effects of L-t-C<sub>6</sub>-Pyr-Cer in combination with gemcitabine (GMZ) in the inhibition of cell growth were also shown in HNSCC cells in vitro (Rossi et al., 2005). However, quantitative supra-additive interaction of these two compounds in vitro or their therapeutic efficacy in the inhibition of HNSCC tumor growth in vivo has not yet been described.

In the present study, the data demonstrate that L-t-C<sub>6</sub>-Pyr-Cer accumulates in mitochondria- and nuclei-enriched fractions in UM-SCC-22A cells, which is consistent with its design to target negatively charged subcellular compartments. In addition, it is shown here that L-t-C<sub>6</sub>-Pyr-Cer inhibits the growth of various HNSCC cell lines at low IC<sub>50</sub> concentrations, independent of their p53 status. Since single agents historically have not been very successful in the management and/or control of head and neck cancers in clinic, synergistic interaction between L-t-C<sub>6</sub>-Pyr-Cer and GMZ in the inhibition of growth of HNSCC cells was shown by isobologram studies. More importantly, the in vivo therapeutic efficacy of L-t-C<sub>6</sub>-Pyr-Cer in combination with GMZ against HNSCC tumor growth was demonstrated using SCID mice harboring UM-SCC-22A xenografts. Moreover, it is shown here that the combination of L-t-C<sub>6</sub>-Pyr-Cer with GMZ results in a significant modulation of telomerase activity, which appears to be regulated at the post-transcriptional level, concomitant with the reduced length of telomeres, in vivo.

## Materials and Methods

**Ceramides and Chemotherapeutic Agents.** The novel water-soluble cationic L-t-C<sub>6</sub>-Pyr-Cer was synthesized by the Synthetic Lipidomics Core at the Department of Biochemistry and Molecular Biology, Medical University of South Carolina (MUSC; Charleston, SC) as described (Z. Szulc, J. Bielawski, and A. Bielawska, unpublished data). Cetyl-pyridinium bromide monohydrate was purchased from Aldrich Chemical Co. (Milwaukee, WI). GMZ was obtained from Eli Lilly (Indianapolis, IN).

**Cell Lines and Culture Conditions.** Human head and neck cancer cell lines UM-SCC-1 (retromolar trigone/floor of the mouth), UM-SCC-14A (SCC of anterior floor of the mouth), and UM-SCC-22A (SCC of hypopharynx) cells were obtained from Dr. Thomas Carey (Department of Otolaryngology/Head and Neck Surgery, University of Michigan, Ann Arbor, MI). Cells were grown in Dulbecco's modified Eagle's medium containing 10% fetal calf serum and 1% penicillin/streptomycin at 37°C in 5% CO<sub>2</sub>. Possible mycoplasma contaminations were monitored regularly by the MycoAlert mycoplasma detection kit (Cambrex Bio Science Rockland, Inc., Rockland, ME) and treated with Plasmocin (InvivoGen, San Diego, CA) when/if necessary.

**Subcellular Fractionation and the Analysis of Ceramide Subspecies by Mass Spectroscopy.** The subcellular accumulation of L-t-C<sub>6</sub>-Pyr-Cer was analyzed by using normal phase high-performance liquid chromatography (LC) and mass spectroscopy (MS). The subcellular fractionations were done using differential centrifugation as described previously (Novgorodov et al., 2005). In short, cells were incubated in a buffer containing 300 mM sucrose, 10 mM HEPES, pH 7.4, 1 mM EDTA, and 0.5 mM phenylmethylsulfonyl

fluoride for 30 min on ice. The cells were then passed through 25-gauge needle for five strokes and centrifuged at 1000g for 10 min, 10,000g for 10 min, and 100,000g for 60 min at 4°C, for collection of the nuclei- and mitochondria-enriched fractions and microsomes, respectively. Each fraction was subjected to Western blotting with cytochrome *c* and lamin B antibodies to confirm the purity of mitochondrial and nuclear fractions.

**MTT Cell Survival Assay and Isobologram Studies.** The concentrations of agents that inhibited cell growth by 50% (IC<sub>50</sub>) were determined from cell survival plots obtained by MTT assays as described previously (Rossi et al., 2005). To determine the supra-additive interaction between L-t-C<sub>6</sub>-Pyr-Cer and GMZ, isobologram plots (Steel and Peckham, 1979) were constructed using IC<sub>50</sub> values of the two agents alone or in combination obtained from MTT assays. A straight line joining points on *x*- and *y*-axes represent the IC<sub>50</sub> concentrations of GMZ and L-t-C<sub>6</sub>-Pyr-Cer alone, and the points representing the IC<sub>50</sub> concentrations of the combination of the two agents are represented as scatter plots on the same graphs. The points that fall within the left of the straight line indicate synergism. The experiments were performed as triplicate in at least three independent experiments. Error bars represent means ± S.D.

**Analysis of Cell Cycle Profiles.** The effects of L-t-C<sub>6</sub>-Pyr-Cer, alone or in combination with GMZ, on the cell cycle profiles of UM-SCC-22A cells at various time points were analyzed in the presence of DNase-free RNase and propidium iodine by flow cytometry as described previously (Rossi et al., 2005). Untreated cells were used as controls.

**Animal Studies.** The use of animals for determining the maximum tolerated dose (MTD), pharmacokinetics, and therapeutic efficacy of L-t-C<sub>6</sub>-Pyr-Cer, alone or in combination with GMZ, were performed according to protocols that were approved by the Institutional Animal Care and Use Committee at the Medical University of South Carolina. The MTD of L-t-C<sub>6</sub>-Pyr-Cer was determined by dose escalation studies. In short, 7-week-old BALB/c mice (Taconic, Germantown, NY) were treated with increasing concentrations of the compound for various time intervals. Possible toxicity of the compound to the vital organs of the animals was analyzed by both gross examination and histopathology. The accumulation of the compound in vital organs and in the serum was also determined by LC/MS as described previously (Koybasi et al., 2004). Blood counts and enzyme assays were performed by Anilytics, Inc. (Gaithersburg, MD).

The role of L-t-C<sub>6</sub>-Pyr-Cer, alone or in combination, in the inhibition of tumor growth in vivo was examined as follows. UM-SCC-22A cell xenografts were obtained by s.c. injection of 4 × 10<sup>6</sup> cells in the posterior flank of the female SCID mice (Taconic). After tumors were grown to at least 100 mm<sup>3</sup> (approximately 2 weeks after implantation), the mice were treated with various chemotherapeutic agents by i.p. injection (alone or in combination) every 4 days for 24 days. Tumor volumes were calculated using the formula: length × width<sup>2</sup> × 0.52. Each experiment included three mice (which harbored two SCC tumors in their flanks) per each treatment, and experiments were done at least in two independent trials. The concentrations of the drugs used in this study were: L-t-C<sub>6</sub>-Pyr-Cer (40 mg/kg), GMZ (40 mg/kg), doxorubicin (1 mg/kg), 5-FU (25 mg/kg), and CP (9 mg/kg). The known MTDs of these compounds are: 80, 120, 2, 25, and 9 mg/kg for L-t-C<sub>6</sub>-Pyr-Cer (this study), GMZ, doxorubicin, 5-FU, and CP, respectively (Inaba et al., 1989; Veerman et al., 1996; van Moorsel et al., 1999; Makino et al., 2001).

**Determination of Telomerase Activity, Human Telomerase Reverse Transcriptase mRNA, and Protein Levels in Tumor Tissues.** Telomerase activity in tissues was measured by the PCR-based telomere repeat amplification protocol (TRAP) using the TRAPeze kit (Invitrogen, Carlsbad, CA), which includes a 36-bp internal control to allow quantification of activity as described previously (Koybasi et al., 2004). The intensity of telomere-specific DNA bands, measured using Quantity One (Bio-Rad, Hercules, CA) software, was normalized to the intensity of internal control bands for each sample on polyacrylamide gels for quantification. The mRNA levels of the

catalytic subunit of telomerase [human telomerase reverse transcriptase (hTERT)] was measured after extraction of total RNA from tumor tissues extracted from the control or treated animals and normalized to mRNA levels of β-actin by the Applied Biosystems 7300 real-time quantitative PCR (Q-PCR) system using TaqMan primer and probe sets for hTERT and β-actin (Applied Biosystems, Foster City, CA). The protein levels of hTERT in HNSCC tumors were determined by Western blot analysis using anti-hTERT rabbit polyclonal antibody (Calbiochem, San Diego, CA) at 1:1000 dilution. The specificity of the antibody was confirmed using extracts obtained from telomerase positive and negative cells by Western blotting.

**Analysis of Telomere Length in Tumor Tissues.** The measurement of telomere length was performed using total genomic DNA samples isolated from tumor tissues of the SCID mice using telomere restriction fragment (TRF) length measurement kit (Roche Diagnostics, Indianapolis, IN) by Southern blotting as described previously (Sundararaj et al., 2004).

**Statistical Analysis.** The statistical analysis of the animal studies to determine the therapeutic efficacy of the compounds in the inhibition of the growth of HNSCC tumors in vivo was performed using Tukey's Student Range Test and SAS-MIXED procedures (SAS Institute, Cary, NC).

## Results

**The Subcellular Localization of L-t-C<sub>6</sub>-Pyr-Cer in UM-SCC-22A Cells.** Exogenous short chain ceramides are known to mediate cell cycle arrest, apoptosis, or senescence in various cancer cells. However, because of their limited solubility and bioavailability, the water-soluble pyridinium-conjugated analogs of ceramides were developed (Novgorodov et al., 2005; Rossi et al., 2005). Since previous data showed that D-e- and L-t-C<sub>6</sub>-Pyr-Cer effectively inhibited the growth of UM-SCC-22A cells with similar IC<sub>50</sub> concentrations (Rossi et al., 2005), L-t-C<sub>6</sub>-Pyr-Cer is used throughout this study because of its high solubility (Z. M. Szulc, J. Bielawski, and A. Bielawska, unpublished data). The chemical structure of L-t-C<sub>6</sub>-Pyr-Cer is shown in Fig. 1A. Pyr-Cer analogs were designed to preferentially localize into negatively charged intracellular compartments, especially mitochondria and nucleus. Therefore, the subcellular accumulation of L-t-C<sub>6</sub>-Pyr-Cer in UM-SCC-22A cells was examined using LC/MS after treatment with 1 μM L-t-C<sub>6</sub>-Pyr-Cer for various time points (1, 3, 6, 12, 24, and 48 h). The results showed that the compound mainly accumulated in the 10,000g fraction, which is enriched mainly in mitochondria, as early as 1 h after treatment, and then it continued to increase to higher levels (1000–3000 pmol/0.1 mg protein) in this fraction between 3 and 48 h of treatment (Fig. 1B). Likewise, L-t-C<sub>6</sub>-Pyr-Cer was detectable in the 1000g fraction, which is enriched in nuclei, within 3 h, and reached to 250 to 2500 pmol/0.1 mg protein levels in this fraction between 6 and 48 h (Fig. 1B). The amounts of the compound in the supernatant or the pellet of 100,000g fractions were either not detectable (at 1–6 h) or minimal (at 12–48 h) in these cells (Fig. 1B). The enrichment of mitochondria and nucleus in 10,000g and 1000g fractions, respectively, were confirmed by Western blotting with antibodies that detect the mitochondrial cytochrome C and nuclear lamin B (Fig. 1C). Taken together, these data demonstrate that L-t-C<sub>6</sub>-Pyr-Cer mainly accumulates in the mitochondria and, to a lesser extent, in the nucleus, within a short time after exposure, as expected by its chemical composition and design.

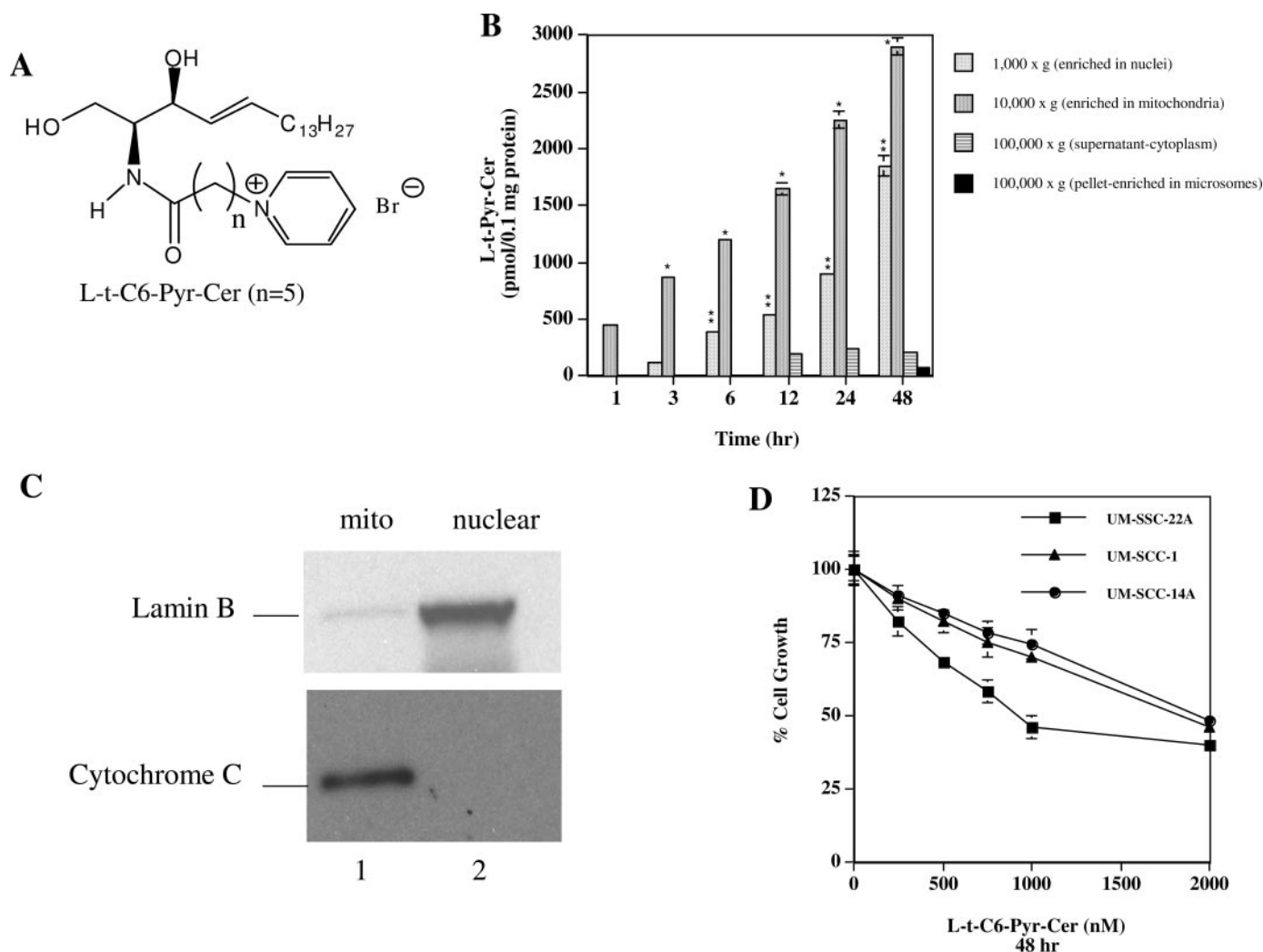


**Fig. 1.** The subcellular accumulation, and growth-inhibitory properties of L-t-C<sub>6</sub>-Pyr-Cer in HNSCC cells. **A**, chemical structure of L-t-C<sub>6</sub>-Pyr-Cer. **B**, subcellular accumulation of L-t-C<sub>6</sub>-Pyr-Cer at 1 to 48 h was detected by LC/MS in UM-SCC-22A cells after differential centrifugation, as described under *Materials and Methods*. **C**, purity of mitochondria- and nuclei-enriched fractions (lanes 1 and 2, respectively) isolated from the UM-SCC-22A cells was analyzed by detecting the levels of cytochrome C (bottom) and lamin B (top) proteins using Western blotting as described under *Materials and Methods*. **D**, growth-inhibitory effects of L-t-C<sub>6</sub>-Pyr-Cer against UM-SCC-22A, UM-SCC-14A, and UM-SCC-1 cells were assessed by MTT assays after treatment of cells with increasing concentrations of the compound for 48 h. Experiments were done in duplicate at least in three independent trials. Error bars, means  $\pm$  S.D. When not seen, error bars are smaller than the diameter of the legends on the graphs. Statistical significance was determined using Student's *t* test, and  $p < 0.05$  (\*) was considered significant.

### The Effects of L-t-C<sub>6</sub>-Pyr-Cer, Alone or in Combination with GMZ, on the Growth of HNSCC Cells in Vitro.

To determine the effects of L-t-C<sub>6</sub>-Pyr-Cer on growth, various cell lines that represent various forms of HNSCC were treated with increasing concentrations of L-t-C<sub>6</sub>-Pyr-Cer for 48 h, and its IC<sub>50</sub>, a concentration that inhibits the growth by 50%, was determined by MTT assays as described under *Materials and Methods*. Consistent with our previous data (Rossi et al., 2005), L-t-C<sub>6</sub>-Pyr-Cer inhibited the growth of human HNSCC cell lines UM-SCC-22A, UM-SCC-1, and UM-SCC14A cells with similar IC<sub>50</sub> concentrations of approximately 1 to 2  $\mu$ M at 48 h (Fig. 1D). Since UM-SCC-1 cells express wild-type p53, whereas UM-SCC-14A cells express mutated p53 (Bradford et al., 2003), their similar IC<sub>50</sub> values for L-t-C<sub>6</sub>-Pyr-Cer suggest that it may regulate cell growth independent of p53 status.

In the clinic, treatment of human HNSCC tumors with a single chemotherapeutic agent has not yielded much success, and therapies, which include the combination of two or more

chemotherapeutic agents, such as 5-FU/CP or taxol/CP, appear to have more promising results (Argiris et al., 2004; Prevost et al., 2005). Therefore, we performed studies to test the growth-inhibitory effects of L-t-C<sub>6</sub>-Pyr-Cer in combination with various conventional chemotherapeutic agents. Previous data (Rossi et al., 2005) showed that the combination of L-t-C<sub>6</sub>-Pyr-Cer with GMZ improved its growth-inhibitory effects against UM-SCC-22A cells, without any quantitative determination of supra-additivity (synergism). In this study, the supra-additive interaction between L-t-C<sub>6</sub>-Pyr-Cer and GMZ in the inhibition of growth of UM-SCC-22A cells was evaluated using quantitative isobologram studies, as described under *Materials and Methods*. The data showed that the combination of L-t-C<sub>6</sub>-Pyr-Cer at its sub-IC<sub>50</sub> values (100, 250, and 500 nM) with increasing concentrations of GMZ for 48 h decreased growth synergistically, as detected by the shift of the IC<sub>50</sub> values of GMZ in the isobologram to the left of the line plot joining the *x*- and *y*-axes that represent the IC<sub>50</sub> of L-t-C<sub>6</sub>-Pyr-Cer and GMZ, respectively (Fig.

2A). In addition, analysis of cell cycle profiles showed that treatment with L-t-C<sub>6</sub>-Pyr-Cer in combination with GMZ (at 500 and 50 nM, respectively, for 48 h) resulted in a cell cycle arrest at G<sub>0</sub>/G<sub>1</sub> and decreased S phase and G<sub>2</sub>/M cell population compared with controls (Fig. 2B). Interestingly, there was no apparent apoptosis in response to this combination treatment in these cells (Fig. 2B).

**Determination of MTD, Pharmacokinetics, and Bioaccumulation of L-t-C<sub>6</sub>-Pyr-Cer in Vivo.** To evaluate the effects of L-t-C<sub>6</sub>-Pyr-Cer in the inhibition of growth in vivo, its MTD was determined by treatment of BALB/c mice with increasing concentrations of L-t-C<sub>6</sub>-Pyr-Cer at 10 to 150 mg/kg for various time points. The data demonstrated that treatment of mice with a single dose of L-t-C<sub>6</sub>-Pyr-Cer at 120 to 150 mg/ml resulted in toxicity resulting in extreme abdominal bloating and intestinal malfunction in some animals after approximately 6 h of treatment (Table 1), whereas treatment with 10 to 80 mg/kg of the compound for 1 to 4 days did not have any detectable toxicity (Table 1). Overall toxicity was determined by gross examination of the animals and histopathological examination of the tissue sections obtained

from brain, heart, lungs, liver, kidney, intestines, and bone marrow (data not shown). Thus, the MTD of L-t-C<sub>6</sub>-Pyr-Cer was determined as 80 mg/kg in mice, which did not cause any detectable toxicity in these animals after either single (Table 1) or multiple (every 4 days for 20 days) cycles of treatment (data not shown).

Next, the pharmacokinetic parameters of L-t-C<sub>6</sub>-Pyr-Cer, such as clearance from the blood and bioaccumulation in various organs, were examined by LC/MS after treatment with the compound at 40 mg/ml (half of the MTD that would be used for the in vivo therapeutic studies) for various time points. As shown in Fig. 3A, the serum levels of the compound reached 4500 to 6500 pmol/0.1 ml serum at 0.5 to 2 h, respectively, and cleared from the serum within 4 h. The levels of the compound increased slightly first in the intestines after 5 min and in the liver after 2 h, which were approximately 600 and 500 pmol/mg protein, respectively (Fig. 3B). The compound started to accumulate mainly in the kidney between 4 and 8 h (Fig. 3B). There was some accumulation in the lungs after 24 h and no significant accumulation in the brain or heart (Fig. 3B). These data suggest that

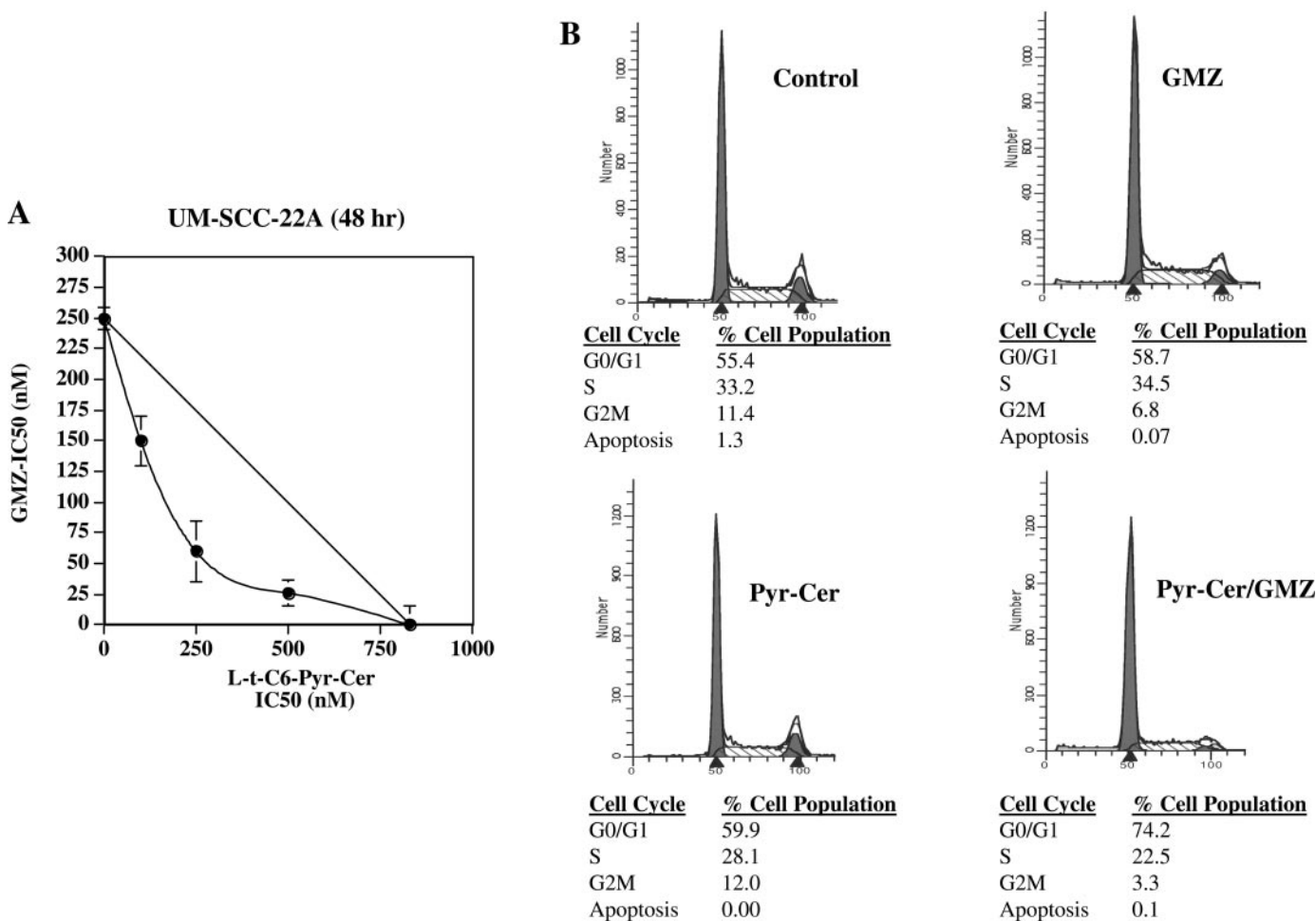


**Fig. 2.** Synergistic effects of L-t-C<sub>6</sub>-Pyr-Cer, in combination with GMZ on the growth and cell cycle profiles of UM-SCC-22A cells. A, synergistic interactions of L-t-C<sub>6</sub>-Pyr-Cer and GMZ in the inhibition of growth were examined by quantitative isobologram studies, as described under *Materials and Methods*. The IC<sub>50</sub> concentrations of GMZ in the presence of increasing concentrations of L-t-C<sub>6</sub>-Pyr-Cer were determined by MTT assays, and the data were plotted in isobolograms. A straight line joining points on x- and y-axes represents the IC<sub>50</sub> concentrations of GMZ and L-t-C<sub>6</sub>-Pyr-Cer alone. The points on the isobologram representing the IC<sub>50</sub> values of GMZ obtained in the presence of 100, 250, and 500 nM L-t-C<sub>6</sub>-Pyr-Cer fell within the left of the straight line, which indicates synergism. The experiments were performed as triplicate in at least three independent experiments. Error bars, means ± S.D. B, effects of L-t-C<sub>6</sub>-Pyr-Cer (500 nM) and GMZ (50 nM), alone or in combination, on cell cycle profiles of UM-SCC-22A cells were determined by flow cytometry after 48 h of treatment, as described under *Materials and Methods*.

TABLE 1

Determination of the MTD of L-t-C<sub>6</sub>-Pyr-Cer in vivo

MTD of L-t-C<sub>6</sub>-Pyr-Cer was determined in dose escalation studies in which BALB/c mice were treated (by i.p. injections) with increasing concentrations of the compound (10–150 mg/kg), dissolved in sterile saline solution, for 24 h. The MTD of the compound was assessed as 80 mg/kg, which did not result in any detectable toxicity in any of the animals. The toxic concentrations of the compound at or >100 mg/kg caused severe abdominal bloating and intestinal malfunction. Possible toxicity of the compound to the vital organs of the animals was analyzed by both gross examination and histopathology.

Group	Dose mg/kg	Total Animals	Mortality %	Toxicity
1	10	4	0	None
2	20	4	0	None
3	40	4	0	None
4	60	4	0	None
5	80	10	0	None
6	100	10	10	N.D.
7	120	10	20	Abdominal bloating
8	150	4	50	Abdominal bloating, intestinal malfunction

N.D., not determined.

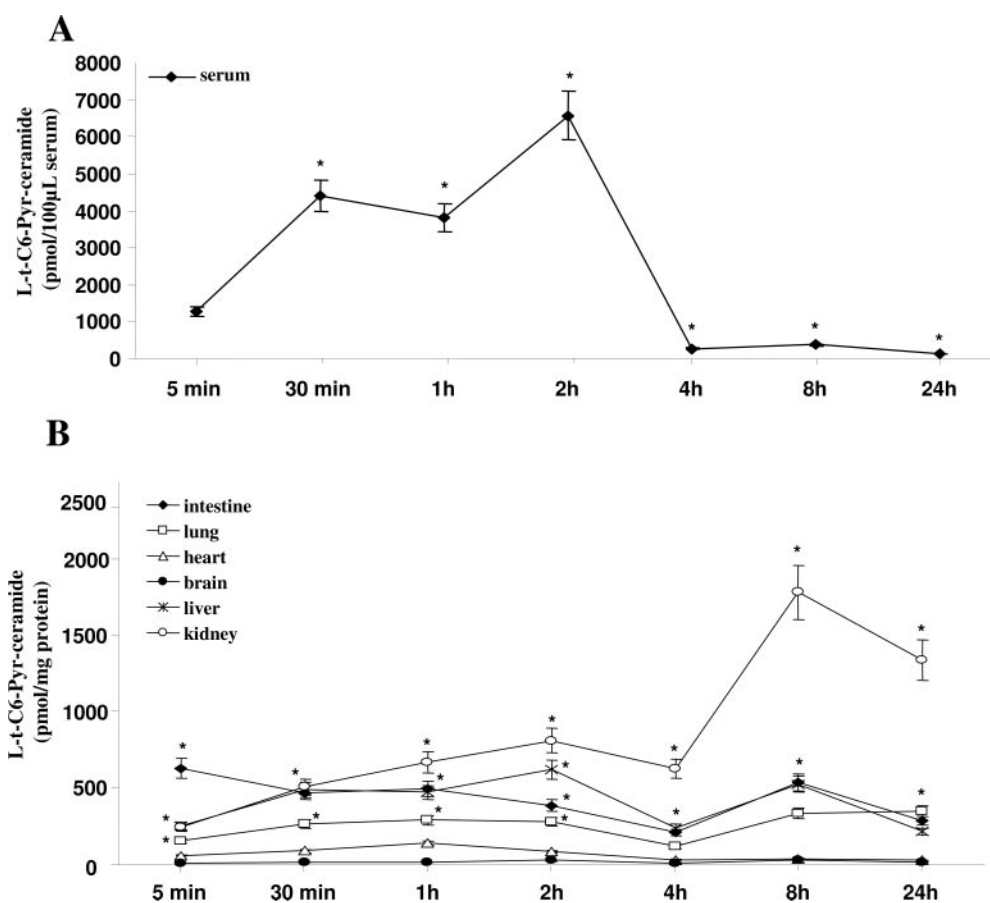


**Fig. 3.** The determination of pharmacokinetic parameters such as clearance from the serum and bioaccumulation in various organs of L-t-C<sub>6</sub>-Pyr-Cer in vivo. Levels of L-t-C<sub>6</sub>-Pyr-Cer in the serum (A) or in the vital organs (B) of the BALB/c mice were measured by LC/MS after i.p. injection of the compound for various time points. The experiments were performed in two independent trials as duplicates. Error bars, means ± S.D. Statistical significance was determined using Student's *t* test, and *p* < 0.05 (\*) was considered significant.

L-t-C<sub>6</sub>-Pyr-Cer circulates through systemic delivery within 2 to 4 h and accumulates in the intestines, liver, and lungs at moderate levels and at high levels in the kidneys within 8 to 24 h, possibly for excretion. These data are consistent with previous studies, which showed the main accumulation of other lipophilic pyridinium cations in the kidneys and excretion in the urine (Pietruck and Ullrich, 1995).

**The Inhibition of HNSCC Tumor Growth by L-t-C<sub>6</sub>-Pyr-Cer Compared with Its Conventional Analog L-t-C<sub>6</sub>-Cer in Vivo.** After determining the MTD, pharmacokinetic, and bioaccumulation parameters, the therapeutic efficacy of L-t-C<sub>6</sub>-Pyr-Cer against HNSCC xenografts, which were developed by s.c. injection of UM-SCC-22A cells to both sides of the flank of the SCID mice, was assessed and compared with the effects of L-t-C<sub>6</sub>-Cer (without the pyridinium

moiety) as described under *Materials and Methods*. After the tumors were established (at least 100 mm<sup>3</sup> in volume), mice were treated with 40 mg/kg ceramides every 4 days for six cycles (total of 24 days). The histopathological analysis of the tumors confirmed that they were SCCs (Fig. 4A). More importantly, as shown in Fig. 4B, the growth of HNSCC tumors was significantly inhibited by L-t-C<sub>6</sub>-Pyr-Cer compared with untreated controls (*p* < 0.001). In addition, these data also showed that the tumor inhibitory effects of L-t-C<sub>6</sub>-Pyr-Cer were approximately 2.5-fold greater than conventional L-t-C<sub>6</sub>-Cer (Fig. 4B).

**The Therapeutic Efficacy of L-t-C<sub>6</sub>-Pyr-Cer in Combination with GMZ in the Inhibition of HNSCC Tumor Growth in Vivo.** Next, the therapeutic efficacy of L-t-C<sub>6</sub>-Pyr-Cer in combination with GMZ against HNSCC tumors

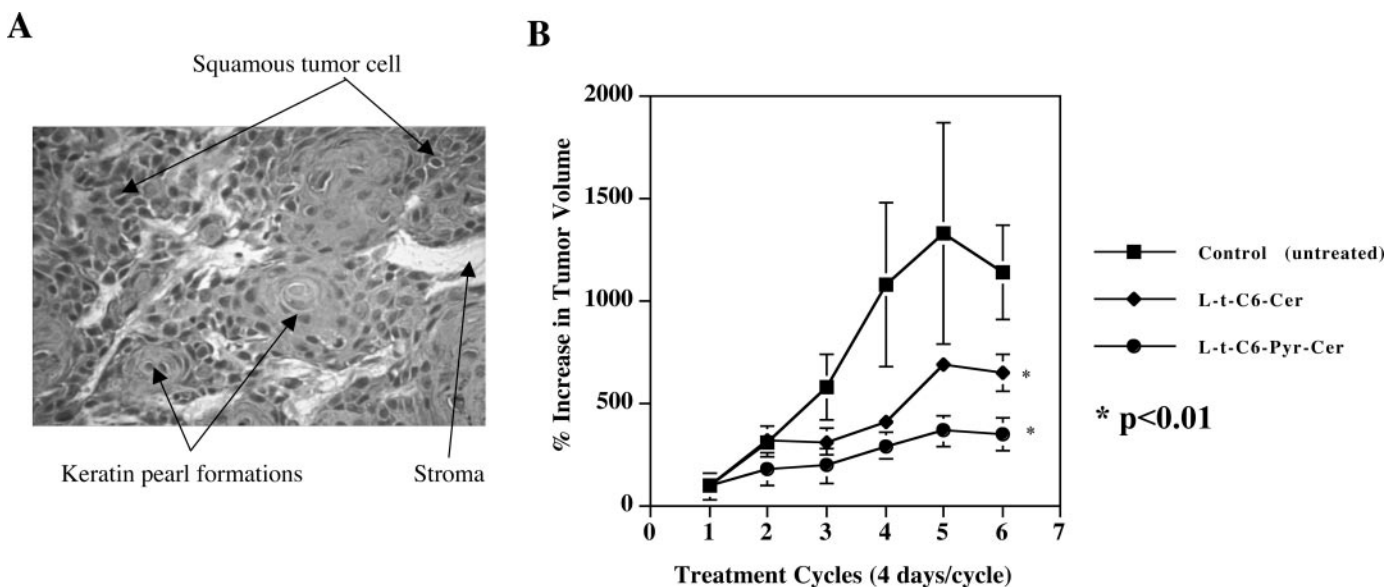


**Fig. 4.** The role of L-t-C<sub>6</sub>-Pyr-Cer compared with its conventional analog L-t-C<sub>6</sub>-Cer in the inhibition of HNSCC tumor growth in vivo. The effects of L-t-C<sub>6</sub>-Pyr-Cer and its conventional analog L-t-C<sub>6</sub>-Cer as single agents were determined in SCID mice harboring the UM-SCC-22A xenografts implanted in both flanks, as described under *Materials and Methods*. A, tumors were confirmed to be squamous cell carcinomas by histopathologic analysis after H&E staining. B, animals were treated with ceramides at 40 mg/kg/each every 4 days for 24 days (six cycles), and untreated mice were used as controls. In these experiments, each group contained three mice, harboring six tumors. Statistical analysis was performed as described under *Materials and Methods*, and  $p < 0.05$  (\*) was considered significant.

was examined in vivo. After the tumors were established (the average initial tumor volumes were 165, 286, 413, 120, and 268 mm<sup>3</sup> for control, GMZ, L-t-C<sub>6</sub>-Pyr-Cer, 5-FU/CP, and L-t-C<sub>6</sub>-Pyr-Cer/GMZ, respectively), the animals were treated with L-t-C<sub>6</sub>-Pyr-Cer or GMZ, alone or in combination, at 40 mg/kg each (at or below their half of MTDs), every 4 days for 24 days. As Fig. 5A shows, treatment with L-t-C<sub>6</sub>-Pyr-Cer or GMZ as single agents caused some inhibition of HNSCC tumor growth in vivo compared with untreated controls. However, the combination of L-t-C<sub>6</sub>-Pyr-Cer with GMZ almost completely inhibited the tumor growth ( $p < 0.01$ ), and the efficacy of this combination was approximately 2.5-fold better than that of 5-FU/CP ( $p < 0.05$ ) (Fig. 5A). Importantly, treatment of animals with L-t-C<sub>6</sub>-Pyr-Cer alone or in combination with GMZ did not cause any significant changes (not more than 5%) in the total body weight of the animals (data not shown). Treatment of SCID mice bearing UM-SCC-22A xenografts with 40 mg/kg cetylpyridinium bromide (without ceramide conjugate) for 4 days was lethal to all animals tested ( $n = 6$ , data not shown). In addition, combination of L-t-C<sub>6</sub>-Pyr-Cer (40 mg/kg) with doxorubicin (1 mg/kg) was toxic to the animals ( $n = 6$ ), killing all the animals at days 2 to 3 of treatment (data not shown).

To confirm the lack of toxicity in response to L-t-C<sub>6</sub>-Pyr-Cer/GMZ treatment, tumors and the vital organs were surgically removed after the completion of the study, and H&E staining of the tissue sections was performed as described. Analysis of the vital organs of the animals treated with L-t-C<sub>6</sub>-Pyr-Cer alone or in combination with GMZ showed no detectable toxicity (data not shown). Blood counts, levels of enzyme activities, and electrolytes in the serum of animals (such as red blood cell and hemoglobin, blood urea nitrogen, creatinine, sodium, magnesium, alanine amino transferase, and amylase) after these treatments were also analyzed (Table 2). There were no detectable abnormalities in these levels, confirming the lack of overall toxicity.

Interestingly, analysis of the levels of L-t-C<sub>6</sub>-Pyr-Cer in HNSCC tumors removed after the completion of the study by LC/MS showed that its accumulation in the tumor site was approximately 2200 pmol/mg when used as a single agent, whereas its levels in the tumors increased approximately 40% (up to 3100 pmol/mg) when combined with GMZ (Fig. 5B). The levels of the compound in the intestines and the liver in the absence of GMZ were approximately 120 and 100 pmol/mg protein, which increased to 1000 and 300 pmol/mg protein in the presence of GMZ. Thus, these data demonstrate that the levels of the compound in tumors were approximately 3- to 6-fold higher than its levels in intestines or liver of the animals, in the absence or presence of GMZ (Fig. 5B). Analysis of the effects of L-t-C<sub>6</sub>-Pyr-Cer, alone or in combination with GMZ, on the endogenous levels of ceramide in tumor site (Fig. 6, A and B), or in the vital organs (data not shown) of the animals showed that treatments with L-t-C<sub>6</sub>-Pyr-Cer, alone or in combination with GMZ, did not cause any sustained elevation of endogenous ceramides compared with untreated controls (Fig. 6, A and B), suggesting that it does not affect the long-term metabolism of endogenous ceramide directly or indirectly. Similar data were also observed for the endogenous sphingomyelin levels, in which no significant changes were observed in response to these treatments compared with untreated controls (data not shown).

**Role of L-t-C<sub>6</sub>-Pyr-Cer in Combination with GMZ in the Regulation of Telomerase in Vivo.** To examine whether the inhibition of HNSCC tumor growth in response to L-t-C<sub>6</sub>-Pyr-Cer, alone or in combination with GMZ, mechanistically involves the inhibition of telomerase in vivo, the levels of enzyme activity, hTERT mRNA, and protein levels were measured in tumor extracts by TRAP, Q-PCR, and Western blotting, respectively, as described under *Materials and Methods*. As shown in Fig. 7A, telomerase activity was inhibited significantly in HNSCC tumors of the animals

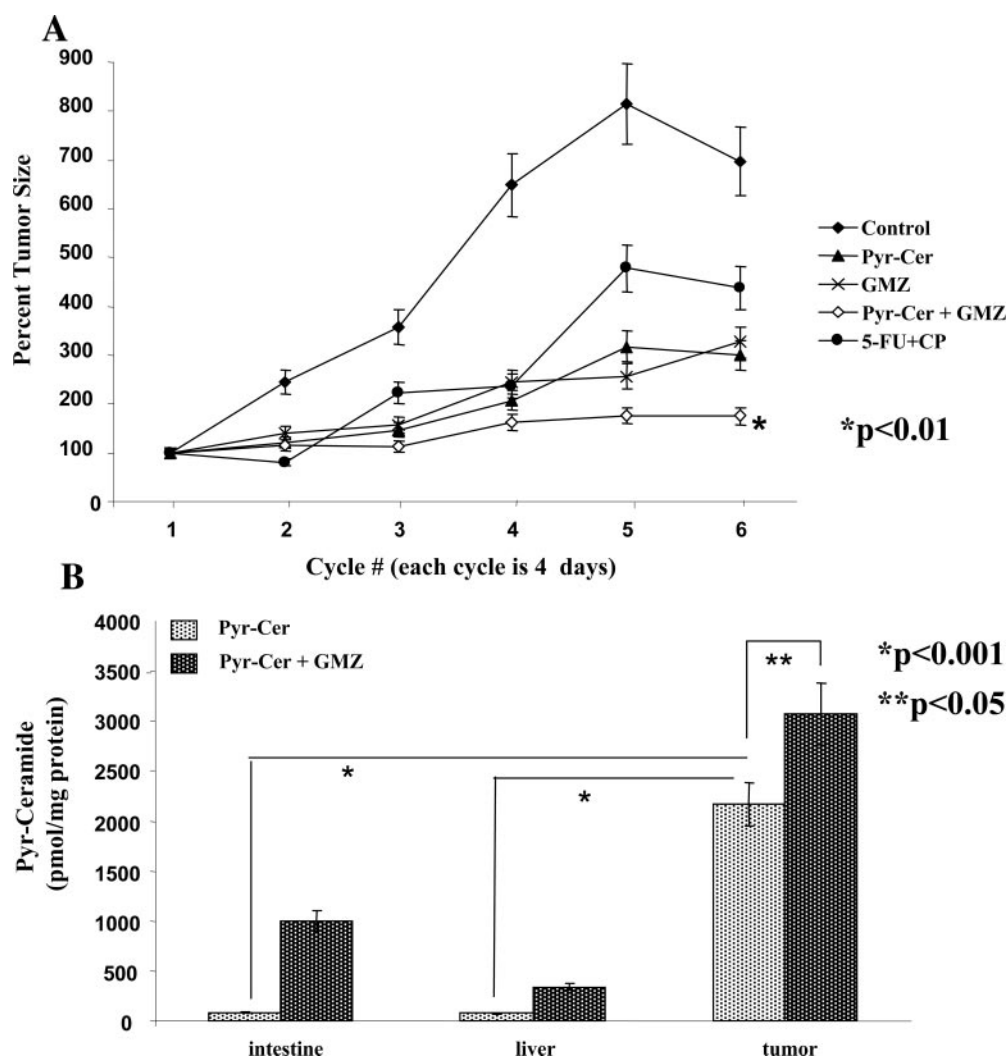


**Fig. 5.** The therapeutic efficacy of L-t-C<sub>6</sub>-Pyr-Cer and GMZ combination in the inhibition of HNSCC tumor growth and/or progression in vivo. A, in vivo therapeutic efficacy of L-t-C<sub>6</sub>-Pyr-Cer in combination with GMZ was determined in SCID mice harboring the UM-SCC-22A xenografts implanted in both flanks, as described under *Materials and Methods*. The animals were treated with L-t-C<sub>6</sub>-Pyr-Cer and GMZ at 40 mg/kg/each every 4 days for 24 days. The therapeutic effects of the 5-FU/CP combination in this HNSCC model were also examined. In these experiments, each group contained six mice, harboring 12 tumors, in this study. Error bars, means ± S.D. *p* values were calculated as described under *Materials and Methods*. B, accumulation of L-t-C<sub>6</sub>-Pyr-Cer in tumor sites or in the intestines and liver was measured by LC/MS after the completion of the study. The effects of GMZ on the levels of L-t-C<sub>6</sub>-Pyr-Cer in these tissues were also examined by LC/MS, as described. Lipid measurements were done in animals (six animals with 12 tumors/group). Error bars, means ± S.D. Statistical significance was determined using Student's *t* test, and *p* < 0.05 (\*) was considered significant.

TABLE 2

Determination of the effects of L-t-C<sub>6</sub>-Pyr-Cer on the blood counts, levels of enzymes, and electrolytes in serum in vivo

The blood counts, levels of serum enzymes, and electrolytes in response to L-t-C<sub>6</sub>-Pyr-Cer (Pyr-Cer) alone or in combination with GMZ in SCID mice were analyzed by Analytics, Inc., as described under *Materials and Methods*. Pyridinium ceramide did not have any detectable effects on these parameters, which were within the normal levels (ranges) in these animals. The data shown here represent the blood work of one of the animals from each group.

Treatment	RBC	Hemoglobin	BUN	Creatinine	Na	Mg	ALT	Amylase
	$1 \times 10^6$ cells/ml	g/100 ml		mg/100 ml		mM/l		U/l
Control	8.0	13.9	19	0.4	145	3.1	24	763
Pyr-Cer	8.4	14.1	23	0.6	142	2.7	52	1589
GMZ/Cer	N.D.	N.D.	36	0.5	147	3.1	23	1526

RBC, red blood cell; BUN, blood urea nitrogen; ALT, alanine aminotransferase; N.D., not determined.

treated with the combination of L-t-C<sub>6</sub>-Pyr-Cer and GMZ by ~60%, which was concomitant with a significant reduction of TRF length (approximately 700 bp) in these tumors compared with untreated controls (Fig. 7B, lanes 5 and 2, respectively). Treatment with L-t-C<sub>6</sub>-Pyr-Cer and GMZ as single agents also caused attrition in telomere length, approximately 500 and 200 bp, respectively, compared with controls (Fig. 7B, lanes 4, 3, and 2, respectively).

Consistent with the proposed mechanisms of action of ceramide in the regulation of telomerase activity at the mRNA levels of hTERT in various human cancer cell lines in vitro, the inhibition of telomerase by L-t-C<sub>6</sub>-Pyr-Cer (Fig. 7A) correlated with decreased levels of hTERT mRNA and protein

expression compared with controls in vivo (Fig. 7, C and D, lanes 3 and 1, respectively). However, although treatment with the combination of L-t-C<sub>6</sub>-Pyr-Cer and GMZ did not cause any detectable changes in the mRNA levels of hTERT (Fig. 7C), its protein levels were significantly inhibited (Fig. 7D, lane 4) in response to this combination, indicating a post-transcriptional regulation. The protein levels of β-actin in these samples were used as loading controls (Fig. 7D, bottom).

Taken together, these data demonstrate, for the first time, that treatment with the combination of L-t-C<sub>6</sub>-Pyr-Cer with GMZ results in a significant inhibition of telomerase activity and decreased telomere length in HNSCC tumors in vivo. Mechanistically, in vivo modulation of telomerase activity by



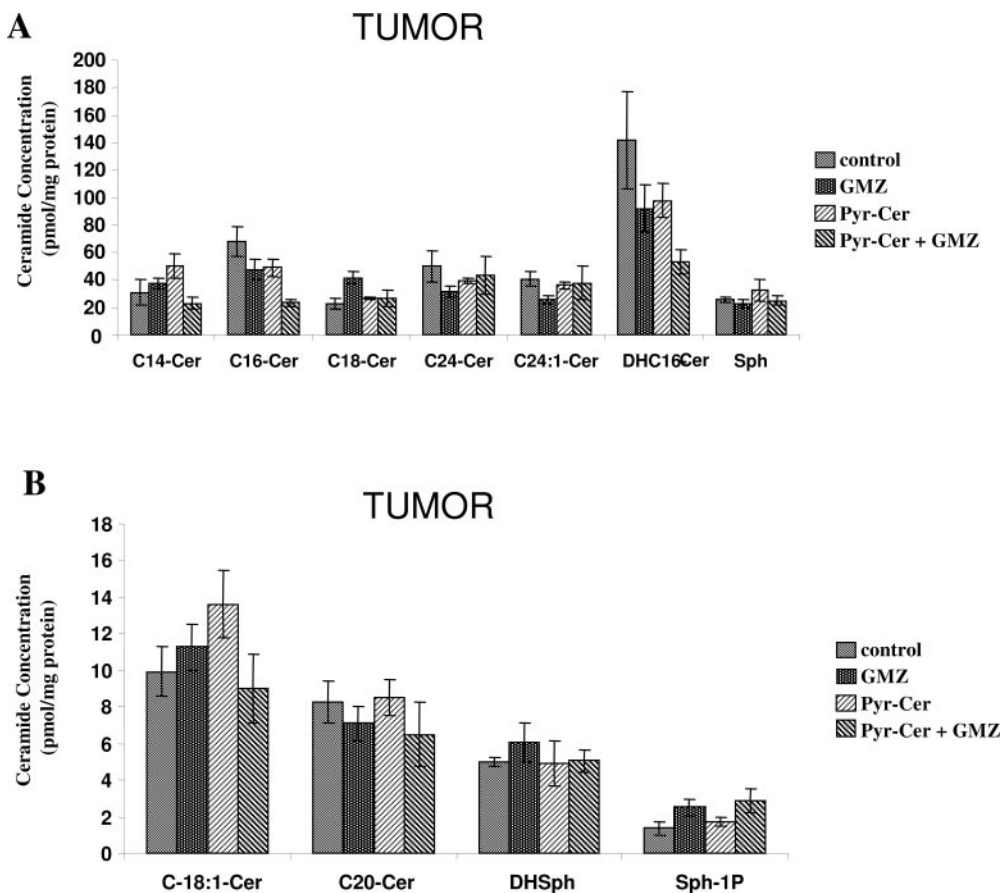


**Fig. 6.** The effects of L-t-C<sub>6</sub>-Pyr-Cer, alone or in combination with GMZ, on the levels of endogenous ceramides and sphingomyelin in HNSCC tumors in vivo. The effects of L-t-C<sub>6</sub>-Pyr-Cer, alone or in combination with GMZ, on the levels of endogenous ceramides (A and B) in HNSCC tumors extracted from SCID mice (summarized in Fig. 5, A and B) were examined by LC/MS. The levels of C14-, C16-, C18-, C24-, C24:1-, dihydro-C16-ceramides, and sphingosine are shown in A, and C18:1- and C20-ceramides, dihydro-sphingosine, and sphingosine-1-phosphate levels are shown in B. Lipid measurements in HNSCC tumors were performed in these animals by LC/MS (*n* = 12/group). Error bars, means ± S.D. There were no significant changes in these levels.

this combination appears to be at the post-transcriptional level, resulting in a significant decrease on the levels of hTERT protein.

## Discussion

In the present study, the growth-inhibitory roles of L-t-C<sub>6</sub>-Pyr-Cer, alone or in combination with GMZ, against HNSCC cells both in vitro and in vivo were examined. It was demonstrated here that L-t-C<sub>6</sub>-Pyr-Cer accumulates mainly in the mitochondria- and nuclei-enriched subcellular fractions, which is consistent with its design and targeting. The data also showed that L-t-C<sub>6</sub>-Pyr-Cer significantly inhibits the growth of various HNSCC cell lines at low IC<sub>50</sub> concentrations, independent of their p53 status. This might be very important for its potential use against variety of cancers, since a majority of cancer cells contain mutated p53 (Don and Hogg, 2004). The supra-additive effects of L-t-C<sub>6</sub>-Pyr-Cer in combination with GMZ on the inhibition of HNSCC cell growth were also determined by quantitative isobologram studies in vitro. More importantly, after preclinical parameters were determined, the data revealed that treatment with L-t-C<sub>6</sub>-Pyr-Cer/GMZ in combination almost completely inhibited tumor growth in the xenograft models of HNSCC in SCID mice, which was much more effective than the effects of 5-FU/CP combination against these tumors. The LC/MS analysis showed that the levels of L-t-C<sub>6</sub>-Pyr-Cer in the tumor site are significantly higher than its levels in the liver and intestines, and, interestingly, the combination with GMZ increased the sustained accumulation of this ceramide. Moreover, the inhibition of HNSCC tumor growth

and/or progression by L-t-C<sub>6</sub>-Pyr-Cer/GMZ was concomitant with the inhibition of telomerase and decrease in telomere length, which are among the cancer-specific nuclear downstream targets of ceramide (Ogretmen and Hanun, 2004). The modulation of telomerase in vivo was regulated at the post-transcriptional level of hTERT protein, leading to a significant decrease in the levels of hTERT in response to this combination.

Because of inherent limitations in the solubility and bioavailability of conventional exogenous ceramides, novel cationic ceramides with high water solubility, cell membrane permeability, and cellular uptake have been designed and synthesized (Novgorodov et al., 2005; Rossi et al., 2005). The presence of the positive charge in the pyridinium ring was designed to target and accumulate these ceramide analogs into negatively charged intracellular compartments, especially mitochondria and nucleus. Previous studies have also demonstrated that the majority of cancer cells acquire high levels of negative charge in their subcellular structures, such as in mitochondria and/or nuclei (Modica-Napolitano and Aprile, 2001), suggesting that pyridinium-ceramides may preferentially accumulate in cancer cells. Indeed, in this study, the accumulation of L-t-C<sub>6</sub>-Pyr-Cer preferentially in mitochondria- and nuclei-enriched fractions was established in UM-SCC-22A cells in vitro, and this was also consistent with the higher accumulation of the compound in the tumor site than in the liver and intestines in vivo. The accumulation of Pyr-Cer in mitochondria has been shown in HepG2 and MCF-7 cells previously, and this caused dramatic alterations in the structures and functions of mitochondria, resulting in

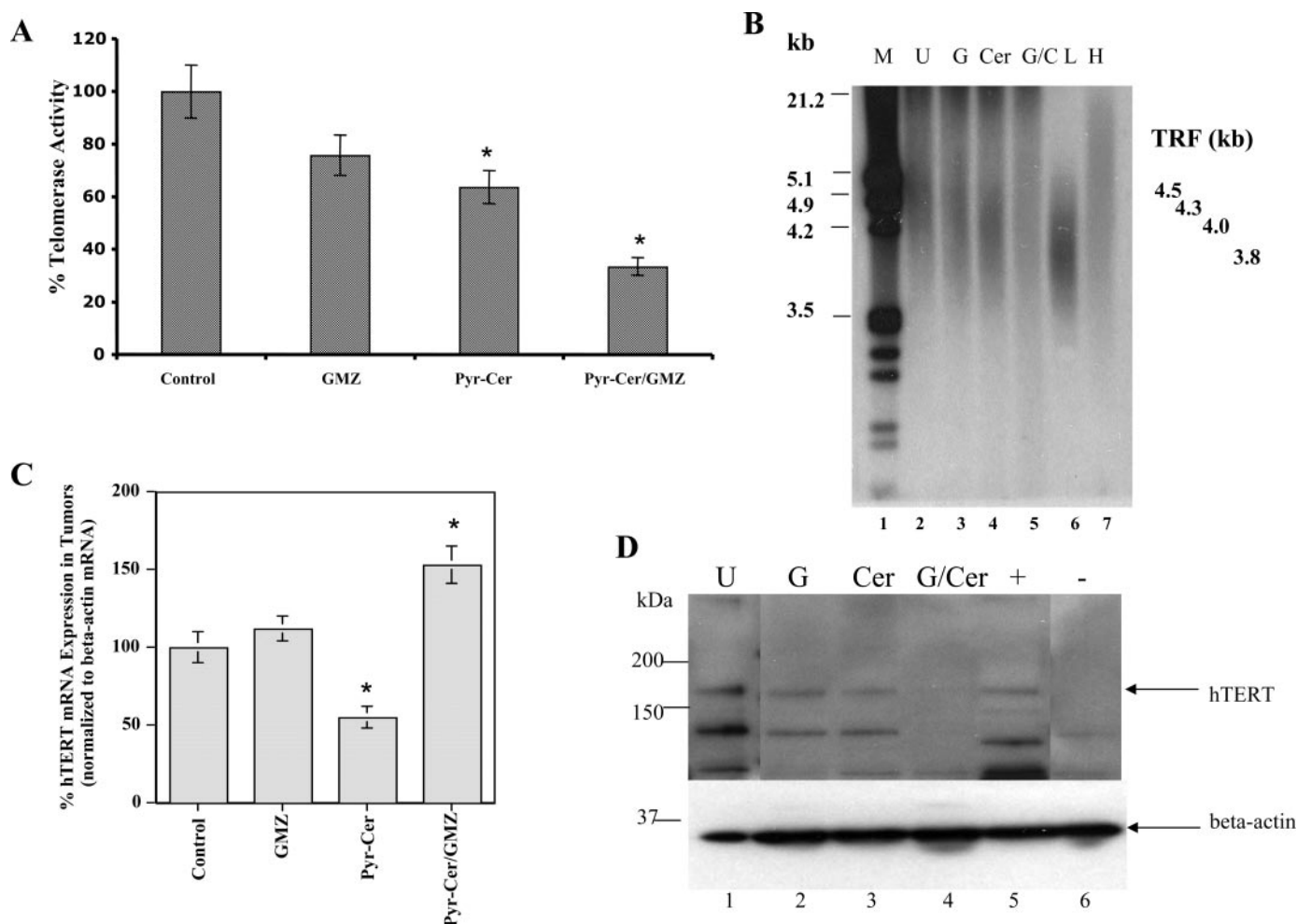


**Fig. 7.** The role of L-t-C<sub>6</sub>-Pyr-Cer, alone or in combination with GMZ, in the inhibition of telomerase in HNSCC tumors in vivo. The role of L-t-C<sub>6</sub>-Pyr-Cer, alone or in combination with GMZ, in the regulation of telomerase activity (A), telomere length analysis (B), the levels of hTERT mRNA (C), and protein (D) in HNSCC tumors extracted from SCID mice after studies summarized in Fig. 5, were examined by TRAP, TRF, Q-PCR, and Western blotting, respectively, as described under *Materials and Methods*. B, DNA samples obtained from tumors treated with GMZ (G), L-t-C<sub>6</sub>-Pyr-Cer (Cer), and the combination of L-t-C<sub>6</sub>-Pyr-Cer with GMZ (G/C, lanes 3–5, respectively) were compared with that of untreated (U) tumors (lane 2). Lanes 5 and 6 contain DNA samples with low (L)- and high (H)-mol. wt. (3.9 and 10.2 kb, respectively) telomeres. In D, the levels of hTERT protein in samples obtained from tumors treated with GMZ (G), L-t-C<sub>6</sub>-Pyr-Cer (Cer), and the combination of L-t-C<sub>6</sub>-Pyr-Cer with GMZ (G/Cer, lanes 2–4, respectively) were determined by Western blot analysis using rabbit polyclonal anti-hTERT antibody and compared with that of untreated (U) tumors (lane 1). Lanes 5 and 6 contain samples from telomerase positive (+) and negative (–) extracts.  $\beta$ -actin levels of these samples were used as loading controls (lanes 1–6, bottom). Statistical significance was determined using Student's *t* test, and  $p < 0.05$  (\*) was considered significant.

apoptotic cell death (Novgorodov et al., 2005). However, effects of L-t-C<sub>6</sub>-Pyr-Cer on the modulation of telomerase and decrease in telomere length in HNSCC in vivo also suggest an important role for its nuclear accumulation. It should be noted also that, in addition to pyridinium-conjugated compounds, there are other compounds, such as F16 and jasmonates, that were shown to accumulate in mitochondria (Fantin and Leder, 2004; Rotem et al., 2005).

The role of exogenous ceramides in mediating antiproliferative functions in various human cancer cells has been demonstrated previously. For example, novel structural analogs of ceramide, such as C<sub>16</sub>-serinol and (2*S*,3*R*)-(4*E*,6*E*)-2-octanoylamidooctadecadiene-1,3-diol (4,6-diene-ceramide), mediated apoptosis in neuroblastoma and breast cancer cells, respectively (Bieberich et al., 2000; Struckhoff et al., 2004). Other ceramide analogs, 5*R*-OH-3*E*-C8-ceramide, adamantyl-ceramide, and benzene-C<sub>4</sub>-ceramide displayed selective growth-inhibitory roles in drug-resistant human breast cancer cell lines (SKBr3 and MCF-7/Adr) (Crawford et al., 2003).

In an alternative approach, delivery of exogenous ceramide in cationic pegylated liposomes increased accumulation of ceramide and enhanced its ability to kill breast cancer cells (Stover and Kester, 2003). The liposomal delivery of exogenous natural ceramide also resulted in the inhibition of phosphorylated Akt and stimulated the activity of caspase-3/7 more effectively than nonliposomal ceramide (Stover and Kester, 2003). Recently, promising in vivo therapeutic efficacy of these pegylated liposomes used for the delivery of exogenous ceramide was shown in breast cancer models (Stover et al., 2005).

Clinical data suggest that head and neck cancers respond better to chemotherapy regimens, which include combinations of two or more anticancer agents (Kroep et al., 1999). Indeed, the conventional chemotherapy for these cancers is the combination of CP with 5-FU or taxol (Kroep et al., 1999). Therefore, in this study, the effects of treatment with L-t-C<sub>6</sub>-Pyr-Cer in combination with GMZ in the inhibition of HNSCC tumor growth and/or progression were examined in

vivo, and the data revealed the superior therapeutic efficacy of this combination over the conventional CP/5-FU treatment. The use of GMZ for the treatment of HNSCC in combination with CP, imatinib, or vinca alkaloids has been reported previously (Kroep et al., 1999; Airoidi et al., 2003; Bruce et al., 2005; Jiang et al., 2005). In addition, GMZ was known to sensitize HNSCC cells to radiation (Aguilar-Ponce et al., 2004). However, these studies reported some toxicity, which limit their therapeutic significance. Since there was no detectable overall toxicity in animals treated with the combination of L-t-C<sub>6</sub>-Pyr-Cer and GMZ, it would be interesting to test the efficacy of combining L-t-C<sub>6</sub>-Pyr-Cer/GMZ with radiotherapy for the treatment of HNSCC in future studies. Interestingly, the data presented here showed that treatment with GMZ enhanced the accumulation of L-t-C<sub>6</sub>-Pyr-Cer significantly in the HNSCC tumors in vivo, which might be very important for their improved efficacy against these tumors. The mechanisms by which GMZ increases in-tumor accumulation of this compound, however, are still unknown and need to be determined.

Moreover, the role of both endogenous and exogenous ceramides in the inhibition of telomerase function in various human cancer cells in vitro has been demonstrated previously (Ogretmen et al., 2001; Wooten and Ogretmen, 2005). Modulation of telomerase by ceramide has been mainly regulated at the transcriptional level of hTERT in human cancer cells in vitro (Wooten and Ogretmen, 2005). However, results presented here showed that treatment with the combination of L-t-C<sub>6</sub>-Pyr-Cer/GMZ inhibited telomerase at the post-transcriptional level in vivo. The mechanisms by which Pyr-Cer/GMZ combination treatment results in decreased levels of hTERT protein in vivo, however, are still unknown and need to be determined. Interestingly, there are data that implicate the involvement of ubiquitin/proteasome pathway for the regulation of hTERT in some cells (Kim et al., 2005). In addition, the role of ceramide in the regulation of c-Myc via increased ubiquitination and proteasome degradation has been shown previously in A549 human lung cancer cells (Ogretmen et al., 2001). Therefore, it would be important to examine whether decreased levels of hTERT protein in response to this combination are regulated by the ubiquitin/proteasome pathway.

In summary, the results presented here suggest that treatment with water-soluble L-t-C<sub>6</sub>-Pyr-Cer in combination with GMZ inhibits HNSCC tumor growth and/or progression with no detectable overall toxicity in vivo, suggesting that the combination of these two compounds might provide alternative strategies for the improved management/control of HNSCC.

#### Acknowledgments

We thank Dr. P. Hall (School of Pharmacy, MUSC) for helping us design animal studies and Dr. T. Carey (University of Michigan) for providing us with the HNSCC cell lines. Analysis of cell cycle profile was performed by the Hollings Cancer Center Flow Cytometry Core Facility at MUSC.

#### References

Aguilar-Ponce J, Granados-Garcia M, Villavicencio V, Poitevin-Chacon A, Green D, Duenas-Gonzalez A, Herrera-Gomez A, Luna-Ortiz K, Alvarado A, Martinez-Said H, et al. (2004) Phase II trial of gemcitabine concurrent with radiation for locally advanced squamous cell carcinoma of the head and neck. *Ann Oncol* **15**:301–306.

Airoidi M, Cattel L, Cortesina G, Giordano C, Passera R, Pedani F, Novello S, Bumma C, and Gabriele P (2003) Gemcitabine and vinorelbine in recurrent head

and neck cancer: pharmacokinetics and clinical results. *Anticancer Res* **23**:2845–2852.

Argiris A, Li Y, Murphy BA, Langer CJ, and Forastiere AA (2004) Outcome of elderly patients with recurrent or metastatic head and neck cancer treated with cisplatin-based chemotherapy. *J Clin Oncol* **22**:262–268.

Bieberich E, Kawaguchi T, and Yu RK (2000) N-Acylated serinol is a novel ceramide mimic inducing apoptosis in neuroblastoma cells. *J Biol Chem* **275**:177–181.

Bradford CR, Zhu S, Ogawa H, Ogawa T, Ubell M, Narayan A, Johnson G, Wolf GT, Fisher SG, and Carey TE (2003) p53 mutation correlates with cisplatin sensitivity in head and neck squamous cell carcinoma lines. *Head Neck* **25**:654–661.

Bruce IA, Slevin NJ, Homer JJ, McGown AT, and Ward TH (2005) Synergistic effects of imatinib (STI 571) in combination with chemotherapeutic drugs in head and neck cancer. *Anticancer Drugs* **16**:719–726.

Cohen EE, Ling M, and Vokes EE (2004) The expanding role of systemic therapy in head and neck cancer. *J Clin Oncol* **22**:1743–1752.

Crawford KW, Bittman R, Chun J, Byun HS, and Bowen WD (2003) Novel ceramide analogs display selective cytotoxicity in drug-resistant breast tumor cell lines compared to normal breast epithelial cells. *Cell Mol Biol* **49**:1017–1023.

Don AS and Hogg PJ (2004) Mitochondria as cancer drug targets. *Trends Mol Med* **10**:372–378.

Fabricius EM, Gurr U, and Wildner GP (2002) Telomerase activity levels in the surgical margin and tumour distant tissue of the squamous cell carcinoma of the head and neck. *Anal Cell Pathol* **24**:25–39.

Fantin VR and Leder P (2004) F16, a mitochondriotoxic compound, triggers apoptosis or necrosis depending on the genetic background of the target carcinoma cell. *Cancer Res* **64**:329–336.

Harrington KJ, Lewanski C, Northcote AD, Whittaker J, Peters AM, Vile RG, and Stewart JS (2001) Phase II study of pegylated liposomal doxorubicin (Caelyx) as induction chemotherapy for patients with squamous cell cancer of the head and neck. *Eur J Cancer* **37**:2015–2022.

Her C (2001) Nasopharyngeal cancer and the Southeast Asian patient. *Am Fam Physician* **63**:1776–1782.

Inaba M, Kobayashi T, Tashiro T, Sakurai Y, Maruo K, Ohnishi Y, Ueyama Y, and Nomura T (1989) Evaluation of antitumor activity in a human breast tumor/nude mouse model with a special emphasis on treatment dose. *Cancer* **64**:1577–1582.

Jemal A, Murray T, Ward E, Samuels A, Tiwari RC, Ghafoor A, Feuer EJ, and Thun MJ (2004) Cancer statistics, 2004. *CA Cancer J Clin* **54**:8–29.

Jiang Y, Wei YQ, Luo F, Zou LQ, Liu JY, Peng F, Huang MJ, and He QM (2005) Gemcitabine and cisplatin in advanced nasopharyngeal carcinoma: a pilot study. *Cancer Invest* **23**:123–128.

Kim JH, Park SM, Kang MR, Oh SY, Lee TH, Muller MT, and Chung IK (2005) Ubiquitin ligase MKRN1 modulates telomere length homeostasis through a proteolysis of hTERT. *Genes Dev* **19**:776–781.

Koscielny S, Eggeling F, Dahse R, and Fiedler W (2004) The influence of reactivation of the telomerase in tumour tissue on the prognosis of squamous cell carcinomas in the head and neck. *J Oral Pathol Med* **33**:538–542.

Koybasi S, Senkal CE, Sundararaj K, Spassieva S, Bielawski J, Ostia W, Day TA, Jiang JC, Jazwinski SM, Hannun YA, et al. (2004) Defects in cell growth regulation by C18:0-ceramide and longevity assurance gene 1 in human head and neck squamous cell carcinomas. *J Biol Chem* **279**:44311–44319.

Kroep JR, Peters GJ, van Moorsel CJ, Catik A, Vermorken JB, Pinedo HM, and van Groeningen CJ (1999) Gemcitabine-cisplatin: a schedule finding study. *Ann Oncol* **10**:1503–1510.

Makino M, Shoji H, Takemoto D, Honboh T, Nakamura S, Kurayoshi K, and Kaibara N (2001) Comparative study between daily and 5-days-a-week administration of 5-fluorouracil chemotherapy in mice: determining the superior regimen. *Cancer Chemother Pharmacol* **48**:370–374.

Modica-Napolitano JS and Aprile JR (2001) Delocalized lipophilic cations selectively target the mitochondria of carcinoma cells. *Adv Drug Deliv Rev* **49**:63–70.

Novgorodov SA, Szulc ZM, Luberto C, Jones JA, Bielawski J, Bielawska A, Hannun YA, and Obeid LM (2005) Positively charged ceramide is a potent inducer of mitochondrial permeabilization. *J Biol Chem* **280**:16096–16105.

Ogretmen B and Hannun YA (2004) Biologically active sphingolipids in cancer pathogenesis and treatment. *Nat Rev Cancer* **4**:604–616.

Ogretmen B, Kravka JM, Schady D, Usta J, Hannun YA, and Obeid LM (2001) Molecular mechanisms of ceramide-mediated telomerase inhibition in the A549 human lung adenocarcinoma cell line. *J Biol Chem* **276**:32506–32514.

Patel MM, Parekh LJ, Jha FP, Sainger RN, Patel JB, Patel DD, Shah PM, and Patel PS (2002) Clinical usefulness of telomerase activation and telomere length in head and neck cancer. *Head Neck* **24**:1060–1067.

Pietruck F and Ullrich KJ (1995) Transport interactions of different organic cations during their excretion by the intact rat kidney. *Kidney Int* **47**:1647–1657.

Prevost A, Merol JC, Aime P, Moutel K, Roger-Liautaud F, Nasca S, Legros M, and Coninx P (2005) A randomized trial between two neoadjuvant chemotherapy protocols: CDDP + 5-FU versus CDDP + VP16 in advanced cancer of the head and neck. *Oncol Rep* **14**:771–776.

Rossi MJ, Sundararaj K, Koybasi S, Phillips MS, Szulc ZM, Bielawska A, Day TA, Obeid LM, Hannun YA, and Ogretmen B (2005) Inhibition of growth and telomerase activity by novel cationic ceramide analogs with high solubility in human head and neck squamous cell carcinoma cells. *Otolaryngol Head Neck Surg* **132**:55–62.

Rotem R, Heyfets A, Fingrut O, Blickstein D, and Shaklai M (2005) Jasmonates: novel anticancer agents acting directly and selectively on human cancer cell mitochondria. *Cancer Res* **65**:1984–1993.

Shabbits JA and Mayer LD (2003) Intracellular delivery of ceramide lipids via liposomes enhances apoptosis in vitro. *Biochim Biophys Acta* **1612**:98–106.

Steel GG and Peckham MJ (1979) Exploitable mechanisms in combined radiotherapy-chemotherapy: the concept of additivity. *Int J Radiat Oncol Biol Phys* **5**:85–93.

Stover T and Kester M (2003) Liposomal delivery enhances short-chain ceramide-induced apoptosis of breast cancer cells. *J Pharmacol Exp Ther* **307**:468–475.

- Stover TC, Sharma A, Robertson GP, and Kester M (2005) Systemic delivery of liposomal short-chain ceramide limits solid tumor growth in murine models of breast adenocarcinoma. *Clin Cancer Res* **11**:3465–3474.
- Struckhoff AP, Bittman R, Burow ME, Clejan S, Elliott S, Hammond T, Tang Y, and Beckman BS (2004) Novel ceramide analogs as potential chemotherapeutic agents in breast cancer. *J Pharmacol Exp Ther* **309**:523–532.
- Sundararaj KP, Wood RE, Ponnusamy S, Salas AM, Szulc Z, Bielawska A, Obeid LM, Hannun YA, and Ogretmen B (2004) Rapid shortening of telomere length in response to ceramide involves the inhibition of telomere binding activity of nuclear glyceraldehyde-3-phosphate dehydrogenase. *J Biol Chem* **279**:6152–6162.
- Tao Z, Chen S, Wu Z, Xiao B, Liu J, and Hou W (2005) Targeted therapy of human laryngeal squamous cell carcinoma in vitro by antisense oligonucleotides directed against telomerase reverse transcriptase mRNA. *J Laryngol Otol* **119**:92–96.
- van Moorsel CJ, Pinedo HM, Veerman G, Vermorken JB, Postmus PE, and Peters GJ (1999) Scheduling of gemcitabine and cisplatin in Lewis lung tumour bearing mice. *Eur J Cancer* **35**:808–814.
- Veerman G, Ruiz van Haperen VW, Vermorken JB, Noordhuis P, Braakhuis BJ, Pinedo HM, and Peters GJ (1996) Antitumor activity of prolonged as compared with bolus administration of 2',2'-difluorodeoxycytidine in vivo against murine colon tumors. *Cancer Chemother Pharmacol* **38**:335–342.
- Wooten LG and Ogretmen B (2005) Sp1/Sp3-dependent regulation of human telomerase reverse transcriptase promoter activity by the bioactive sphingolipid ceramide. *J Biol Chem* **280**:28867–28876.

---

**Address correspondence to:** Dr. Besim Ogretmen, Medical University of South Carolina, Department of Biochemistry, 173 Ashley Avenue, Charleston, SC 29424. E-mail: ogretmen@musc.edu

---